Inhibitive Effect of Cetyltriphenylphosphonium Bromide on C-steel Corrosion in HCl Solution

*S. Abd El Wanees[1,3, *], Mohammed I. Alahmdi[3], S.M. Rashwan[2], M. M. Kamel[2], and M.G. Abd Elsadek[4]*

[1] Chemistry Department, Faculty of Science, Zagazig University, Zagazig, Egypt
[2] Chemistry Department, Faculty of Science, Seuz Canal University, Ismailia, Egypt
[3] Chemistry Department, Faculty of Science, Tabuk University, Tabuk, Saudi Arabia
[4] General petroleum company "GPC", Western desert fields, Egypt.
[*]E-mail: s_wanees@yahoo.come

Cetyltriphenylphosphonium bromide (CTPPB) was investigated as a corrosion inhibitor for C-steel in 0.5 M HCl using chemical and electrochemical techniques, as well as, surface examination by SEM. The data indicated that CTPPB gives good inhibition effect and the inhibition mechanism is based on the adsorption process forming a barrier layer film that protect the metal from acid attack. The adsorption is found to obey Langmuir model. The effect of temperature was studied. The inhibition efficiency increased by increasing inhibitor concentration and decreased with temperature. Some thermodynamic parameters for adsorption process are deduced and discussed.

1. INTRODUCTION

The study of corrosion inhibition of C-steel took great efforts of scientists and researchers especially in acidic media. The practical importance of this aspect is found in many fields, among of which, the acid pickling of iron and steel, electro-polishing, chemical cleaning and processing, metallic ores production, oil recovery and petrochemical industries. Hydrochloric acid is consider as an important mineral acid used in previous fields [1–5]. The effective inhibitor is generally required in these processes to control the metal distortion process and acid consumption. Actually, the effective acid corrosion inhibitors are bulky organic molecules that carry heteroatoms such as N, S or O atoms and give higher inhibition efficiency [6–10].

Among the effective inhibitors with high protection efficiency and environmentally save are the surface-active, surfactants that are used as inhibitors for corrosion of steel [11-15]. In addition, the low price of these materials and the relative ease of preparation prefer the using of surfactants towards
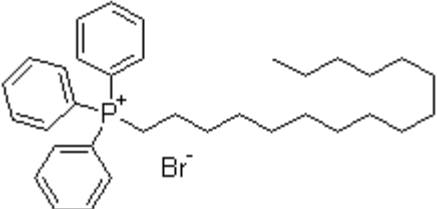
the corrosion of steel [16–20]. Previous studies attributed the inhibitive effect of surfactants in aqueous solution to the adsorption process through the active centers on the metallic surface, which is physico- or chemi- sorption type or both together. The adsorption of the surfactant molecules alter the corrosion resisting property of the tested material [21–24]. The adsorption process depends on many factors among of which are the nature and the type of charge on the metallic surface, the type of corrosive solution, the structure of the added inhibitor and the nature of its interaction with the metallic surface [24].

The aim of the present study is to highlight the inhibitive effect of a pure and cheap surfactant, cetyltriphenylphosphonium bromide (CTPPB) towards the corrosion of C-steel in 0.5 M HCl, using chemical and electrochemical techniques. Weight loss, hydrogen gas evolution and potentiodynamic polarization techniques, as well as, scanning electron microscope, SEM, investigation. The effect of temperature on the dissolution and inhibition process is studied. The adsorption mechanism and the inhibition efficiency of CTPPB are investigated and some thermodynamic parameters are calculated and discussed.

2. MATERIALS AND METHODS.

2.1. Materials

Table 1. Molecular structure, molecular formula (M.F.) and molecular weight (M.W.) of cetyltriphenylphosphonium bromide (CTPPB).

Molecular structure	M.F.	M.W.
	$C_{34}H_{48}BrP$	567.62

C-steel used in forms of a rod as a working electrode and sheets had the following composition (wt.%): 0.12% C, 0.5% Mn, 0.17% Si, 0.06%S, 0.046% P and the remainder iron. Steel coupons are prepared with dimensions of 2.0 cm x 7.6 cm x 1.2 cm were used for weight loss, hydrogen evolution measurements and SEM investigation. For potentiodynamic polarization and electrochemical impedance spectroscopy cylindrical C-steel rods with surface area of 0.42 cm^2 are used. Prior to each run, the sample was abraded with 280, 400, 600, 800 and 1200 grades of emery papers. The specimens were washed thoroughly with distilled water, degreased and dried with ethanol before being weighed and immersed in 100 ml of the test solution.

Cetyltriphenylphosphonium bromide (CTPPB) is used as a cationic surfactant, Table 1, was purchased from Aldrich Chemical Co. The corrosive solution (0.5 M HCl) was prepared by appropriate dilution of analytical grade 37% HCl with bi- distilled water.

2.2. Weight loss method

The C-steel samples were allowed to stand for the desired time in a closed beaker containing 100 ml 0.5 M HCl solution with and without the required concentration of CTPPB. Experiments were carried out in duplicate and the mean weight losses value were reported. The procedure of weight loss study was similar to that reported before [25-27].

2.3. Hydrogen evolution method

For the hydrogen evolution technique, the used C-steel sample are similar to that used in weight loss measurements. The procedure of H_2 measurements was similar to that reported before [25, 26]. A 100 ml of the corrosive or the inhibitive solution was introduced into the reaction vessel, containing C- steel coupon. The volume of the evolved of hydrogen gas was followed at different times.

2.4. Electrochemical measurements

A conventional three electrode electrochemical cell system is used for electrochemical experiment. A Pt wire was used as an auxiliary electrode. The reference electrode was saturated calomel electrode (SCE), while C-steel electrode was the working electrode. Before each run, the working electrode was abraded and prepared as used before [11, 25-27]. Before starting polarization, the prepared electrode was left in the test solution until E_{st} is reached. All electrochemical measurements were performed using a laboratory potentiostat (Volta lab 40 PGZ301, France). The potentiodynamic polarization measurements were obtained by changing the electrode potential automatically from -800 to -220 mV vs SCE, at a scan rate of 0.2 mVs^{-1}, at 25 ºC.

The surface coverage (θ) and inhibition efficiencies (η %) at different CTPPB concentration, are calculated using the following equations [25, 26] :

$$\theta = \left(1 - \frac{I_{inh}}{I_{free}} \right) \tag{1}$$

$$\eta \% = \left(1 - \frac{I_{inh}}{I_{free}} \right) 100 \tag{2}$$

where I_{inh} and I_{free} are the corrosion current densities in 0.5 M HCl with and without CTPPB inhibitor, respectively.

2.5. Electrochemical impedance spectroscopy (EIS)

Impedance measurements were carried out in frequency range from 100 kHz to 0.5 Hz with amplitude of 5 mV peak-to-peak using AC signals at open circuit potential. The experimental impedance were analyzed and interpreted based on the equivalent circuit model [11].

2.6. Scanning electronic microscope (SEM)

Two of C-steel specimens were abraded with emery papers then were washed with bi-distilled water and acetone. After immersion for a period of 30 min in 0.5 M HCl without and with 1×10^{-3} M CTPPB, at 25°C, the C-steel specimens were pack up, cleaned with distilled water, dried using a cold air blaster for investigation under SEM using A Jeol JSM-5400 instrument.

3. RESULTS AND DISCUSSION

3.1. Weight loss measurements:

The corrosion behavior of the examined metal in an aqueous environment is generally characterized by the extent to which it dissolves in the solution. Fig 1 depicts the data of weight loss-time curves of the examined C-steel in aqueous solution of 0.5 M HCl devoid of- and containing different concentrations of CTPPB, at 25°C. It seems clear that, the weight loss of C-steel coupons in the absence and presence of CTPPB inhibitor varies linearly with time. The loss in weight in presence of inhibitor is much lower than that obtained in free acid solution. This loss in weight becomes more lower as CTPPB concentration is increased. In additions, the linear fitting of weight loss- time relation confirms that the dissolution of C-steel in the corrosive solution is accompanied by the formation of soluble corrosion products [27].
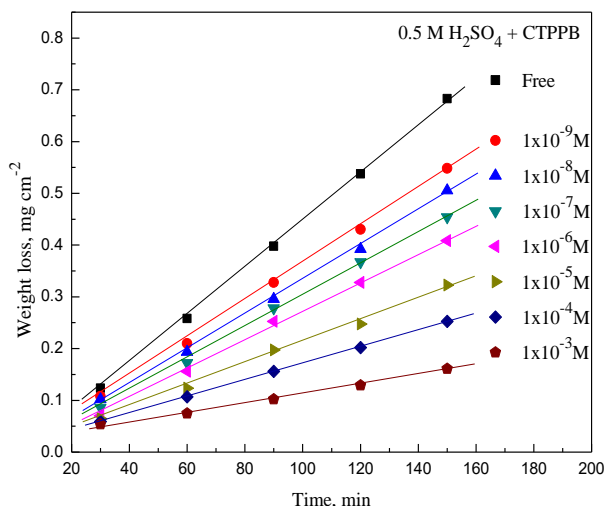

Figure 1. Weight loss-time curves for C-steel in 0.5 M HCl devoid of and containing different concentrations of the CTPPB.

Mathematical equations based on the previous literature can be used to express the experimental data of mass loss by some of corrosion parameters such as, corrosion rate (*r*), surface coverage (*θ*) and inhibition efficiencies (*η* %), as following [25, 26]:

$$r = \left(\frac{\Delta W}{St} \right) \tag{3}$$

$$\theta = \left(\frac{r_o - r_i}{r_o}\right) \tag{4}$$

$$\eta\% = \left(\frac{r_o - r_i}{r_o}\right) 100 \tag{5}$$

where ΔW is the mass loss, r_o and r_i are the rate of corrosion in 0.5 M HCl without and with CTPPB inhibitor, respectively, S is the total surface area in cm^2 and t is the immersion time, in min. The calculated values of corrosion characteristic, r, θ, η % are listed in Table 2. It is clear that CTPPB inhibitor retards the dissolution of C-steel in 0.5 M HCl, by decreasing the corrosion rate, which becomes lower by increasing the inhibitor concentration. The inhibition efficiency, η %, is increased to take maximum value (81.4%) with 1×10^{-3} M CTPPB.

Table 2. Values of corrosion rate, r, θ and η % at different concentrations of CTPPB in 0.5 M HCl, at 25°C.

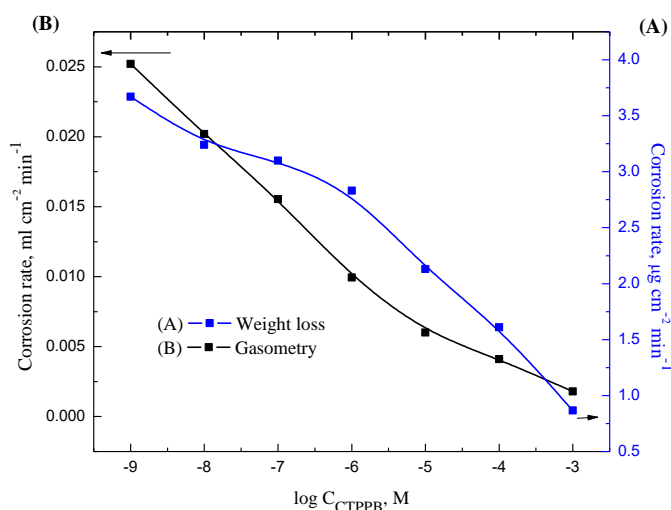| CTPPB concentration, M	Mass loss method			Hydrogen evolution method		
	r, µg cm^{-2} min^{-1}	θ	η %	r, ml cm^{-2} min^{-1}	θ	η %
Free	4.660	--	--	0.032	--	--
1×10^{-9} M	3.670	0.212	21.2	0.0252	0.213	21.3
1×10^{-8} M	3.350	0.281	28.1	0.0202	0.369	36.9
1×10^{-7} M	3.100	0.335	33.5	0.0155	0.516	51.6
1×10^{-6} M	2.830	0.393	39.3	0.0099	0.691	69.1
1×10^{-5} M	2.130	0.543	54.3	0.0072	0.775	77.5
1×10^{-4} M	1.610	0.665	65.5	0.0411	0.872	87.2
1×10^{-3} M	0.867	0.814	81.4	0.0282	0.912	91.2

Figure 2. Variation of rate of corrosion with log C$_{CTPPB}$ for C-steel in 0.5 M HCl: (A) weight loss method and (B) gasometry method.

Fig 2A depicts the **v**ariation of rate of corrosion, r, of C-steel with the logarithm of CTPPB concentration. S-shaped relation is obtained, confirming that the inhibition of CTPPB on C-steel surface can be attributed to the adsorption process [25, 26].

3.2. Hydrogen evolution

C-steel coupons were performed in 0.5 M HCl devoid of- and containing different concentrations of CTPPB, at 25°C. The concentration of the inhibitor is varied between 1×10^{-9} and 1×10^{-3} M. Fig 3 depicts the increase in the volume of the evolved H_2 gas on C-steel surface with the immersion time. It is noteworthy to see that, there is an induction period before the sudden increase in the volume of the evolved H_2 gas. This period is known as an incubation period, which is required to remove any pre-immersion oxide film on the metal surface and start metal dissolution [25, 26]. After incubation period, the volume of the H_2 gas evolved increases linearly with time due to the possible anodic dissolution of the bare metal surface according to the reaction:

$$Fe \rightarrow Fe^{+2} + 2e^{-} \qquad (6)$$

The accompanied cathodic reaction consumes the electrons released in the anodic reaction is the overall H_2 reaction:

$$2H^{+} + 2\,e^{-} \rightarrow H_2 \qquad (7)$$

However, it is noteworthy to see that the rate of corrosion is determined from the linear relation between the volume, V, of H_2 evolved in ml/cm^2, and the immersion time, t, in minute, Fig 3, according to the relation:

$$V = r\,t \qquad (8)$$

where r is the slope of the straight lines, (V- time relation). The data shows that the rate of dissolution of C-steel, under the prevailing experimental conditions, decreases as the CTPPB concentration is increased according to sigmoidal S-shaped curve, Fig 2B.
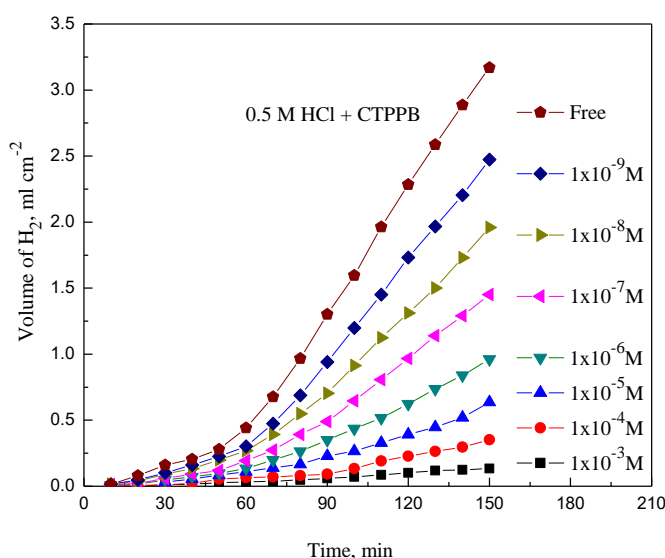
Figure 3. Volume-time curves for C-steel in 0.5 M HCl devoid of and containing different concentrations of CTPPB.

This behavior gives as an indication that the inhibition of C-steel corrosion by CTPPB is suggested to depend on the adsorption of the inhibitive molecules on the metallic surface [25, 26]. The values of the surface coverage (θ) and inhibition efficiencies (η %) at different concentrations of

CTPPB, are calculated from the values of corrosion rate (*r*) as shown before [25, 26], Table 2. It is clear that the values of θ and η % takes higher values as the CTPPB concentration is increased, as due to the increase in the amount of the adsorbed CTPPB molecules on metallic surface.

3.3. Potentiodynamic polarization measurements

The curves of Fig. 4 depicts the potentiodynamic polarization curves for C-steel in 0.5M HCl without and with additions of various concentrations of cetyltriphenylphosphonium bromide (CTPPB) inhibitor, at 25ºC. It is clear that, each of the cathodic and anodic polarization curves in presence of CTPPB inhibitor are suppressed. CTPPB increases the over-voltage of each of cathodic and anodic processes, causing parallel displacement of Tafel lines into the more active and noble directions, respectively. This behavior could prove that the mechanism of hydrogen evolution reaction is activation-controlled process. In addition, both the hydrogen evolution and the anodic dissolution mechanisms are not altered by presence of CTPPB inhibitor [28]. Also, it is noted that the anodic and cathodic Tafel slopes take little change in presence of CTPPB suggesting that the adsorption of CTPPB molecules on the anodic and cathodic sites is controlled by a mixed-type, by blocking of both the active anodic and cathodic reaction sites [29].
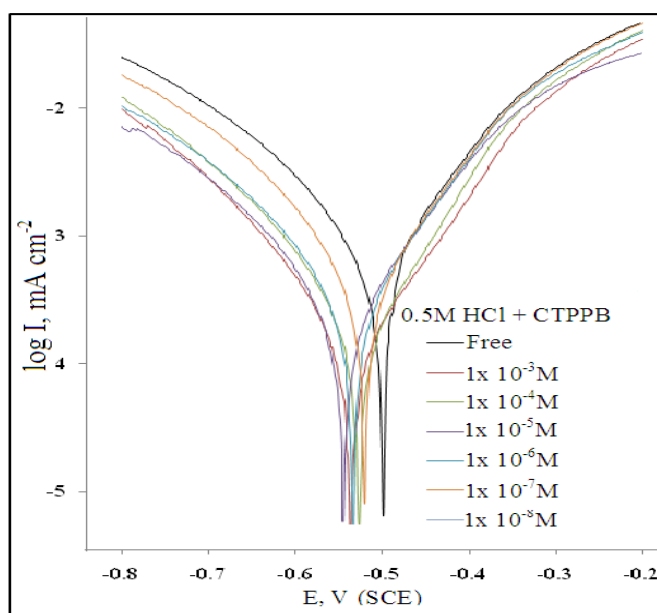

Figure 4. E-log I curves for C-steel in 0.5M HCl devoid of and containing different concentrations of CTPPB, at 25$^{\text{o}}$C

Table 3 shows the electrochemical corrosion parameters, such as, corrosion potential, E_{corr}, corrosion current density, I_{corr}, cathodic Tafel slope, β_c, anodic Tafel slope, β_a, of the corrosion process in the absence and presence of different concentrations of CTPPB. The η % obtained from potentiodynamic polarization measurements are increased with increasing CTPPB concentrations and follow the same sequence to those deduced from weight loss and gasometry measurements.

Table 3. The electrochemical corrosion parameters of C-steel in 0.5 M HCl devoid of and containing of different concentrations of CTPPB, at 25°C.

CTPPB concentration, M	$-E_{corr.}$ mV (vs SCE)	I_{corr} mAcm^{-2}	$-\beta_c$ mVdec^{-1}	β_a mVdec^{-1}	θ	η %
Free	501.2	1.0365	198.6	288.9	--	--
1x10^{-7} M	522.7	0.7527	183.5	148.8	0.274	27.4
1x10^{-6} M	536.3	0.615	190.2	150.3	0.407	40. 7
1x10^{-5} M	547.1	0.4402	192.2	149.7	0.575	57.5
1x10^{-4} M	529.4	0.3622	169.9	130.2	0.651	65.1
1x10^{-3} M	538.5	0.2266	149.6	128.3	0.781	78.1

3.4. Electrochemical impedance spectroscopy (EIS)

The inhibition performance of an inhibitor on a metallic surface depends on many factors among of which is the chemical structure of the inhibitor, the nature of the metal, and also on the experimental conditions such as the immersion time, pH of the solution, as well as, the concentration of the adsorbent [30, 31]. The effect of cetyltriphenylphosphonium bromide (CTPPB) on the corrosion of C-steel in HCl was also studied by EIS method to confirm the results obtained by other used methods. The curves of Fig.5 depicts the Nyquist plots for C-steel in 0.5 M HCl solution devoid and containing different concentrations CTPPB inhibitor, at 25°C. The impedance spectra were measured at the corresponding open-circuit potentials. The impedance spectra show the existence of the single semicircle proving the single charge transfer process accompanying the metallic dissolution step, which is uninfluenced by the presence CTPPB. It is noteworthy to see that the curves of the Nyquist plots plotted in Fig 5 are not perfect semicircles. This behavior could be interpreted as stated before to the frequency dispersion effect as due to electrode roughness and inhomogeneity effect[32, 33]. To analyze the impedance spectra, the equivalent circuit given in Fig 6 is used. In this circuit, R_s refers to the solution resistance between the steel electrode and the reference electrode while R_{ct} represents charge-transfer resistance and C_{dl} represents the electrochemical double layer capacitance. Generally, the presence of inhibitor enhances R_{ct} and decreases C_{dl}. The lowering in C_{dl} values in presence of inhibitor can be suggested to the presence of a protective film formed as due to adsorption of the inhibitor on metal surface [32-35].

The values of the charge transfer R_{ct} are calculated for different of CTPPB concentrations by the high and low frequencies using the equation [36]:

$$R_{ct} = [Z_{real} \text{ (at low frequency)} - Z_{img} \text{ (at high frequency)}] \qquad (9)$$

The values of the C_{dl} obtained from the analysis of Nyquist diagram at the maximum frequency f_{max} at the maximum imaginary impedance Z_{max} and the resistance of charge transfer R_{ct} (diameter of high frequency loop) using the equation [37]:

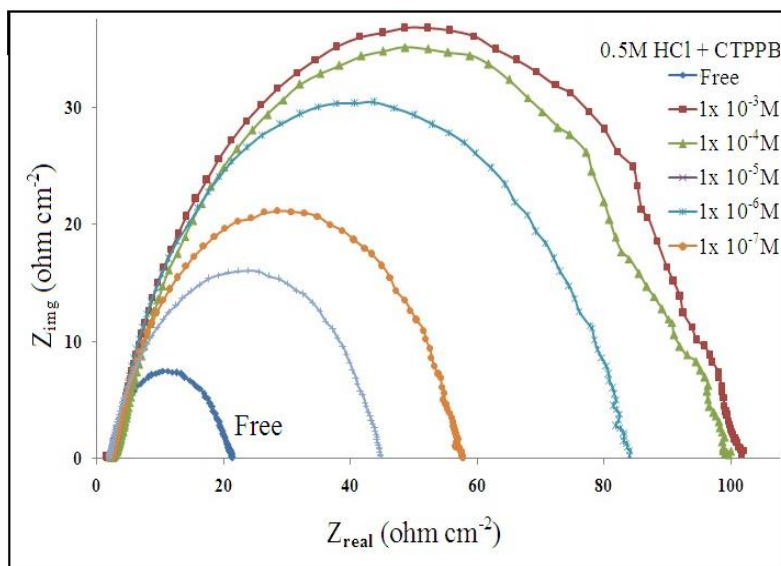$$C_{dl} = \frac{1}{2\pi f_{max} R_{ct}} \qquad (10)$$

Figure 5. The Nyquist plot for C-steel in 0.5 M HCl devoid of and containing different concentrations of CTPPB, at 25°C.

The values of surface coverage (θ) and the percentage inhibition efficiency (η' %) in presence of CTPPB, are calculated from the data of R_{ct} values using the equations [38]:

$$\theta = \left(\frac{R_{ct,inh} - R_{ct}}{R_{ct,inh}} \right) \tag{11}$$

$$\eta' \% = \left(\frac{R_{ct,inh} - R_{ct}}{R_{ct,inh}} \right) 100 \tag{12}$$

where $R_{ct,\ inh}$ and R_{ct} are the charge transfer resistance calculated with and without CTPPB inhibitor, respectively, in 0.5M HCl. The calculated data of the electrochemical parameters of EIS measurements are tabulated in Table 4. It is noted, from the data of this table, the increase the charge transfer resistance, R_{ct} and the decrease in the double layer capacitance, C_{dl}, with increasing CTPPB concentration. This behavior prove that the inhibition of C-steel corrosion in HCl solution by the action of CTPPB inhibitor can be related to the adsorption process, forming a protective layer on metal surface [36]. In addition, the values of inhibition efficiency (η' %) in presence of CTPPB takes higher values with increasing inhibitor concentration to reach 80.9 % with 1×10^{-3}M CTPPB.
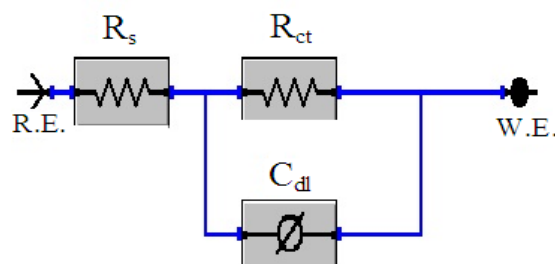

Figure 6. Equivalent circuit compatible with the experimental impedance data.

Table 4. EIS data of C-steel in 0.5 M HCl with and without different concentrations of CTPPB, at 25°C.

CTPPB concentration, M	C_{dl}, $\mu F cm^{-2}$	R_{ct}, $\Omega\ cm^2$	θ	η %
Free	124.3	20.22	--	--
1×10^{-7}	123.4	25.77	0.2499	25.0
1×10^{-6}	103.7	42.95	0.4248	42.5
1×10^{-5}	88.8	56.63	0.5628	56.3
1×10^{-4}	54.27	65.69	0.6539	65.4
1×10^{-3}	49.05	81.10	0.8085	80.9

3.5. Adsorption isotherm

Many general adsorption isotherms provided by many scientists, such as, Temkin, Langmuir, Frumkin, Frundlich, Bockris-Swinkels and Flory-Huggins isotherms, are used to fit the experimental data. The confirmed adsorption isotherm was found to obey Langmuir type. This type of isotherm can be represented by the mathematical equation [39]:

$$\frac{C_{inh}}{\theta} = \frac{1}{K_{ads}} + C_{inh} \tag{13}$$

where C_{inh} is the CTPPB concentration and K_{ads} is the adsorbability constant of the adsorption process, θ is the surface coverage calculated by equation using geometry measurements.

Plotting of C_{inh}/θ versus C_{inh} gives a straight-line relation, Fig 7, confirming Langmuir adsorption isotherm. The corresponding linear regression parameters are listed in Table 5. Each of the linear correlation coefficient and slope are approximately equal to one, suggesting that the adsorption of CTPPB on C-steel surface obeys Langmuir adsorption isotherm. In addition, the value of the adsorbability constant, K_{ads} can calculated from the inverse of the intercept value, according to equation 13. The large value of K_{ads} is an indication of strong adsorption of CTPPB on C-steel surface.
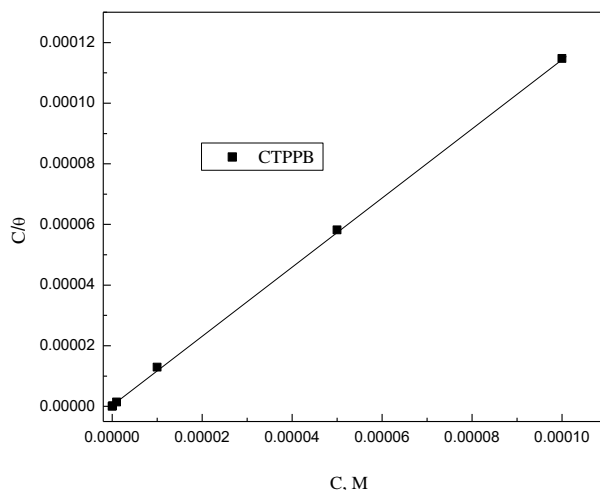

Figure 7. Langmuir's adsorption isotherm of CTPPB on C-steel in 0.5M HCl, at 25°C.

The standard free energy of adsorption, ΔG°, can be calculated from the value of the adsorbability constant, K_{ads}, according to the equation [39]:

$$K_{ads} = \frac{1}{55.5} \exp\left(\frac{-\Delta G^\circ}{RT}\right) \qquad (14)$$

where T is the absolute temperature, 55.5 is the concentration of water expressed in molar value and R is the gas constant equal to 8.314 $Jk^{-1}mol^{-1}$. The calculated ΔG° value is tabulated in Table 5. The negative value of ΔG° gives an indication that the adsorption of CTPPB on C-steel surface is a spontaneous process. As is already well established, values of ΔG°_{ads} up to -20 kJ/mol are consistent with electrostatic interaction between the charged molecules and the charged metal surface (phsi-sorption). Values of ΔG°_{ads} more negative than to -40 kJ/mol involving sharing or transfer of electrons from the organic inhibiting species to the metal surface to form a metal bond [40, 41].

Table 5. The value of linear correlation coefficient, r^2, adsorbabilty constant K_{ads} and free energy of adsorption, ΔG° for CTPPB on C-steel surface in 0.5 M HCl, at 25°C.

r^2	K_{ads}, mol^{-1}	ΔG°, kJ/mol
0.9999	2.55×10^6	-46.5

3.6. Scanning electron micrographs (SEM):

Scanning electron micrographs for C-steel samples after immersion for a period of 30 min in the corrosive solution in the absence and presence of 1x 10^{-3} M CTPPB are investigated. Fig 8(A&B) represented micrographs for C-steel after immersion in (A) 0.5 M HCl and (B) 0.5 M HCl + 1 x 10^{-3}M CTPPB. Investigation of the SEM micrographs taken in 0.5 M HCl solution in absence of inhibitor explores that the surface C-steel sample was strongly attacked with deep cavities on surface surrounded by corrosion products, (Fig 8A). Investigation of the morphology of SEM taken in presence of CTPPB inhibitor, Fig (8B), shows that the surface of C-steel becomes coated by cracked cover layer, compared with that of free acid [42]. This proves that the CTPPB inhibitor is adsorbed on metal surface forming a thick protective layer at 1x10^{-3}M inhibitor, hindering the corrosion process [43].

On the other hand, Fig 9(A&B) and Table 6 show the SEM complementary EDS analysis of the corrosion products formed on the steel electrode surface immersed in 0.5M HCl solution for 30 min in absence, Fig 9A and in presence of 1 x 10^{-3} M of CTPPB, Fig 9B. Inspection of Fig 9(A&B) and Table 6 indicates that the atomic percent of Fe in the scanned area (which is connected with steel corrosion) decreases relatively in presence of the added organic additives CTPPB than in their absence. This could be attributed to the effective action of the added CTPPB as an inhibitor for corrosion of steel.
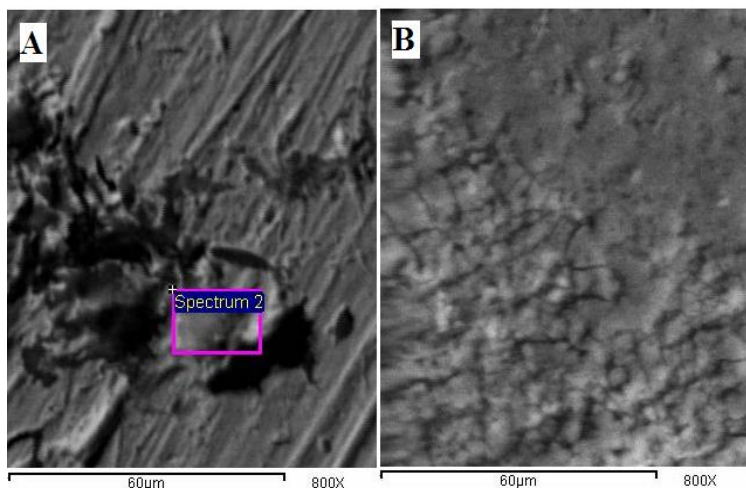
Figure 8. Scanning electron micrographs, SEM for C-steel after immersion for 30 min in (A) 0.5 M HCl and (B) 0.5 M HCl + 1x 10^{-3} M CTPPB, at 25 ºC.
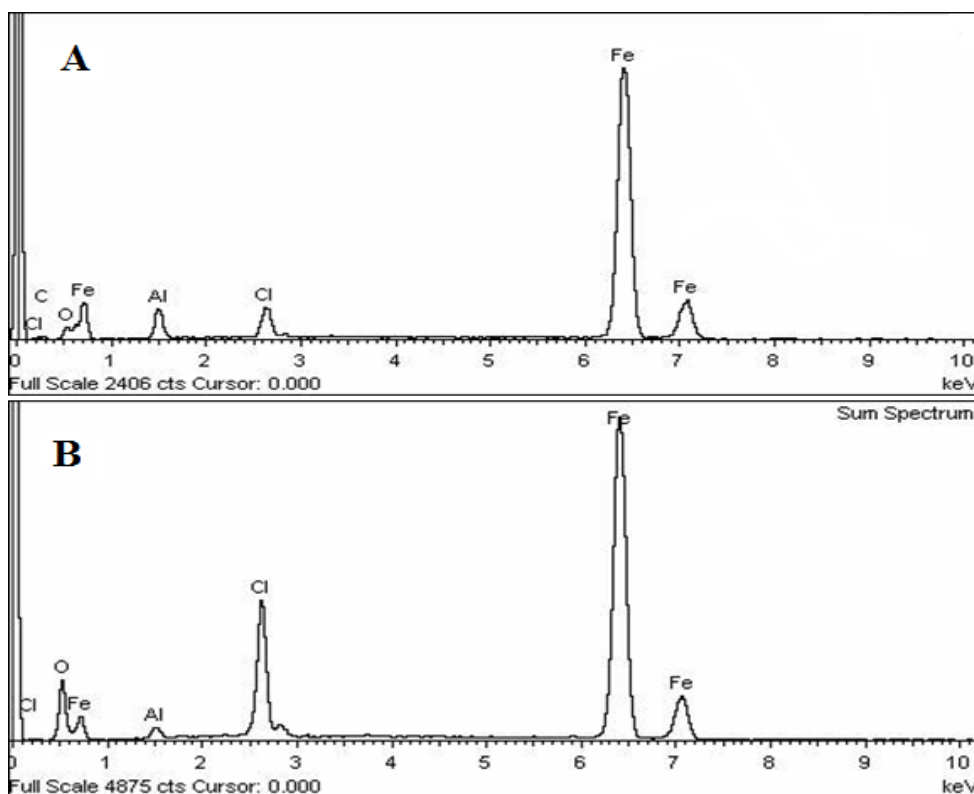

Figure 9. EDS analysis of corrosion products formed on steel surface in: (A) 0.5 M HCl in (A) and (B) 0.5 M HCl + 1x10^{-3}M CTPPB.

Table 6. Elemental analysis (% weight) of C-steel after immersion for 30 minutes in 0.5 M HCl with and without 1 x 10^{-3} M of CTPPB.

(% Mass)	Fe	C	O	Cl	Al	P
Blank	74.03	7.79	6.79	4.21	7.18	--
CTPPB	43.70	--	24.67	28.44	2.96	0.23

3.7. Effect of temperature

The increase in temperature of the corrosive solution is considered to accelerate the destruction of most of metals and metal-alloys. The effect of temperature on the rate of corrosion of C-steel in solutions of 0.5 M HCl devoid of- and containing different concentrations CTPPB (1×10^{-9} to 1×10^{-3} M) is studied by weight loss method.
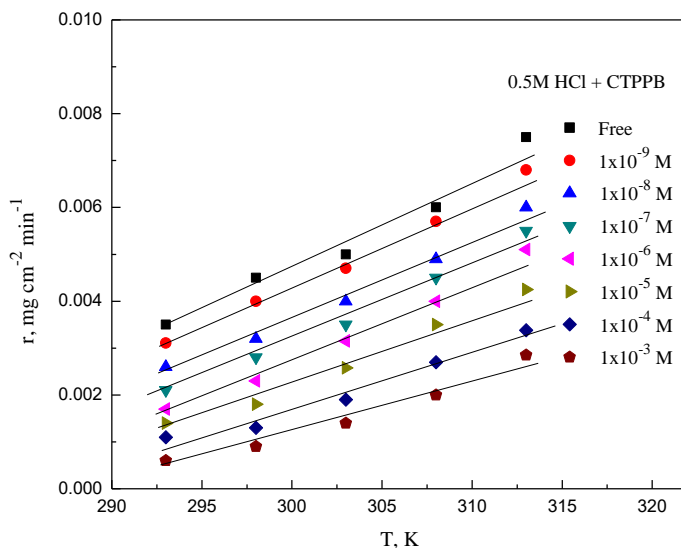

Figure 10. Variation of the corrosion rate of C- steel in 0.5M HCl solutions devoid of and containing different concentrations of CTPPB.

Table 7. The values of the constants *a* and *b* of equation 15.

0.5M HCl + CTPPB	a, µg cm^{-2} min^{-1}	b, µg cm^{-2}
Free	2.0×10^{-4}	-0.055
1×10^{-9} M	1.59×10^{-4}	-0.044
1×10^{-8} M	1.54×10^{-4}	-0.043
1×10^{-7} M	1.50×10^{-4}	-0.041
1×10^{-6} M	1.49×10^{-4}	-0.044
1×10^{-5} M	1.48×10^{-4}	-0.042
1×10^{-4} M	1.18×10^{-4}	-0.034
1×10^{-3} M	0.94×10^{-4}	-0.027

The corresponding corrosion rates calculated in the absence and presence of CTPPB are plotted against temperature, as depicted in Fig 10. The data revealed that increasing the temperature increases the rate of corrosion of C-steel surfaces. Straight-line relation is obtained satisfying the equation:

$$r = a + b \, T \tag{15}$$

where *a* and *b* are constants, Table 7. The constant *b* represents the rate of decrease in the corrosion rate/unit decade of temperature.

In addition, the dependence of the rate of corrosion on temperature can be expressed by Arrhenius and transition state equations [26–28]:

$$\log r = \frac{-\Delta E_a}{2.303RT} + \log A \tag{16}$$

$$\frac{r}{T} = \frac{R}{Nh} \exp\left(\frac{\Delta S_a}{R}\right) \exp\left(\frac{-\Delta H_a}{RT}\right) \tag{17}$$

where r is the corrosion rate, ΔE_a is the apparent activation energy, T is the absolute temperature, A is a frequency factor, ΔH_a is the apparent enthalpy of activation, ΔS_a is the apparent entropy of activation, h is Planck's constant and N is the Avogadro's number, respectively.

The values of $\log r$ (in mg cm^{-2} min^{-1}) obtained at different temperatures, confirm linear relation with 1/T, Fig 11. The slope of the obtained relation is used to calculate the Arrhenius activation energy, ΔE_a, in the absence and presence of inhibitor, Table 8. It is clear that the values of ΔE_a in the presence of inhibitor are higher than that obtained with free acid solution and become more higher as the CTPPB concentration is increased. The increase in ΔE_a values is suggested to the increase in the energy barrier due to formation of a protective film that isolate the C-steel surface from the corrosive acidic solution.

A plot of $\log (r/T)$ versus $(1/T)$ gives straight lines, Fig 12, confirming equation 17, with a slope equal to $[-\Delta H_a/2.303R]$ and an intercept of $[\log (R/Nh) + \Delta S_a/2.303R]$. The calculated values of ΔH_a and ΔS_a are given in Table 8. The positive sign of enthalpy reflect the endothermic nature of steel dissolution process meaning that the dissolution of steel is difficult under such conditions[42, 44]. As can be seen from Table 8, the values of each of ΔE_a and ΔH_a take lower values with free acid solution than that of inhibitive solutions. Moreover, the increase in the inhibitor concentration leads to an increase in the value of ΔE_a, indicating strong adsorption of the inhibitor molecules at the C-steel surface. From the other point of view, the values of $-\Delta S_a$, Table 8, in presence of CTPPB inhibitor is lower that that of free acid solution and it decreased more as the inhibitior concentration is increased. This can be explained on the basis that, in the free acid solution, the transition state of the rate-determining step represents a more order arrangement relative to the initial state. From the other point of view, it indicated that disordering is decreased on going from reactant to activated complex representing an association neither dissociation step [45].

Table 8. The values ΔE_a, ΔH_a and ΔS_a for corrosion of C-steel in 0.5 M HCl without and with different concentrations of CTPPB.

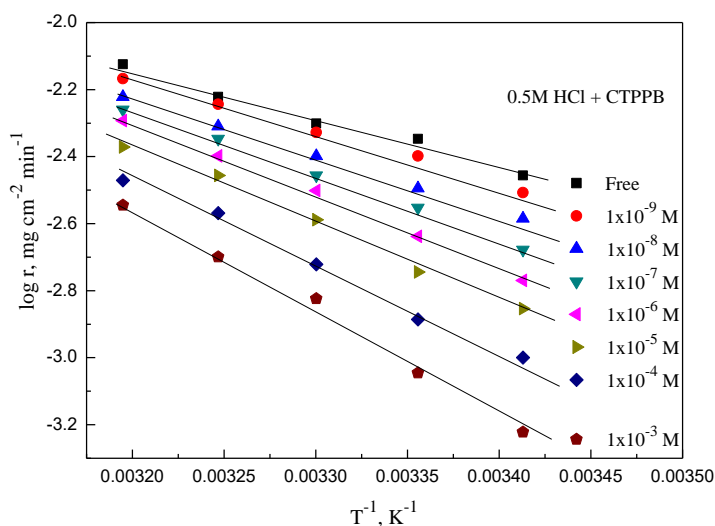| 0.5 M HCl + CTPPB	ΔE_a, kJ mol^{-1}	ΔH_a, kJ mol^{-1}	$-\Delta S_a$, J mol^{-1}
Free	25.9	25.1	206
1x10^{-9} M	29.3	26.8	201
1x10^{-8} M	32.0	29.5	193
1x10^{-7} M	36.6	34.1	179
1x10^{-6} M	42.0	39.5	163
1x10^{-5} M	44.0	41.5	158
1x10^{-4} M	48.3	47.4	140
1x10^{-3} M	59.8	57.2	111

Figure 11. Arrhenius plots (log *r* vs. 1/*T*) for corrosion of C-steel in 0.5M HCl devoid of and containing different concentrations of CTPPB.
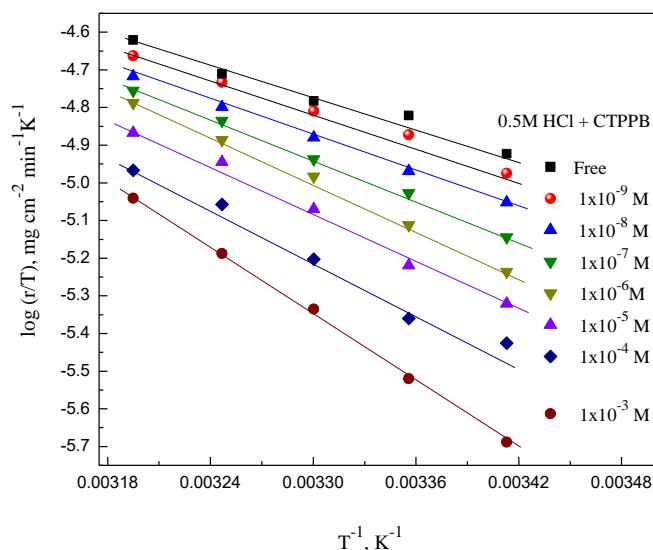

Figure 12. Transition-state plots (log *r/T* vs. 1/*T*) for corrosion of C-steel in 0.5M HCl devoid of and containing different concentrations of CTPPB.

3.8. Inhibition mechanism

Discussion of the inhibition process by many surfactants through adsorption mechanism at the metallic surface is described early [46, 47]. The adsorption process can be interpreted due to interaction of free electrons located on hetero-atoms and/or that of π-bonds of C-H skeleton of inhibitor molecule with empty d-orbitals of atoms on metal surface forming a protective film [48–50]. However, the inhibition process of CTPPB may be achieved by two ways. The first one could be related to physico-sorption due to Van Der Waals force. The main hydrophilic part $-^+P(C_6H_5)_3Br$ may be directed to C-steel surface leaving the hydrophobic tail ($-C_{16}H_{33}$) directed to the bulk of solution.

From the other point of view, Halo-ions carried by ionic surfactant has an important controlling role in adsorption process by shifting the zero charge potential positively, leaving the metallic surface carrying negative charge [51]. In acid solution, the CTPPB can easily, become positively charged. Electrostatic attraction between the positive charge of surfactant molecule and the negatively charged C-steel surface easy to form a barrier film avoiding acid attack for C-steel surface. However, the decrease in inhibition efficiencies at higher temperatures can be attributed to the desorption process from metallic surface [52].

4. CONCLUSIONS

The corrosion rate of C-steel in 0.5 M HCl in presence of different concentrations of CTPPB is examined by different chemical and electrochemical techniques. The study indicated that:

1. CTPPB acts as an effective inhibitor by forming energy barrier film on C-steel surface. It behaves as a mixed-type inhibitor for C-steel in HCl.

2. Inhibition efficiency increases as the concentration of CTPPB is increased.

3. The adsorption of CTPPB on C-steel surface follows Langmuir model-type.

4. The increase in ΔE_a values in presence of higher concetration of CTPPB is related the high adsorption effect of the inhibitor on the metallic surface.

5. The adsorption of CTPPB on C-steel surface in HCl could be attributed to the chemisorption type.

6. The value ΔG°_{ads} is -46.5 kJ/mol explain the spontaneous adsorption process with sharing or transfer of electrons from the CTPPB species to chemical bond with metallic surface.

References

1. L. Garverick, Corrosion in the Petrochemical Industry, ASM International, Materials Park, OH (1994) p.178.
2. A. Chetouani, K. Medjahed, K. E. Benabadji, B. Hammouti, S. Kertit and A.Mansri, *Prog. Org. Coat.*, 46(2003)312.
3. H. Ashassi-Sorkhabi, M.R. Majidi and K. Seyyedi, *Appl. Surf. Sci.*, 225(2004)176.
4. H. Ashassi-Sorkhabi, B. Shaabani and D.Seifzadeh, *Electrochim. Acta*, 50 (2005) 3446.
5. F. Bentiss and M. Lagrence, *J. Appl. Electrochem.*, 31(2001)41.
6. S. Kertit, J. Aride, A. Ben-Bachir, A. Sghiri, A. Elkoly and M. Etman, *J. Appl. Electrochem.*, 19 (1989) 83.
7. L. Wang, *Corros. Sci.* 43 (2001) 1637.
8. M. Abdallah, H.E. Meghaed and M. Sobhi, *Mater. Chem. Phys.*, 118 (2009) 111.
9. X. L. Cheng, H.Y. Ma, S. Chen, R. Yu, X. Chen and Z.M. Yao, *Corros. Sci.*, 41 (1999)321.
10. M.A. Hegazy, M. Abdallah and H. Ahmed, *Corros. Sci.*, 52 (2010) 2897.
11. M. A. Hegazy, *J. Mol. Liq.*, 208 (2015)227.
12. A. S.El- Tabei, M. A. Hegazy, *Chem. Eng. Commun.*, 7 (2015)851.
13. H.N. Shubha, T.V. Venkatesha, M. K. Pavithra, M.K. Punith Kumar, *Progress in Org. Coat.*,90(2016) 267.
14. M. A. Hegazy, A. S.El- Tabei, *J. Surfactant. Deterg.*, 16(2013)221.

15. D.N. Singh and A.K. Dey, *Corrosion NACE*, 49 (1993) 594.
16. G. Banerjee and S.N. Malhotra, *Corrosion NACE*, 48 (1992) 10.
17. S.T. Arab and E.A. Noor, *Corrosion NACE*, 49 (1993) 122.
18. L.A. Raspi, Nickel *Corrosion NACE*, 49 (1993) 821.
19. Y. Chen, Y. Wang, G. Zhang, *Daily Chem. Ind.*, 2 (1986) 56.
20. L. Shi, H. Song, *Daily Chem. Ind.*, 1 (1987) 9.
21. J.M. Bastidas, P. Pinilla, J.L. Polo, S. Miguel, *Corros. Sci.*, 45 (2003) 427.
22. A.E. Bolzan, I.B. Wakenge, R.C.V. Piatti, R.C. Salvarezza, A.J. Arvia, *J. Electroanal. Chem.*, 501 (2001) 241.
23. E. Stipnisek-Lisac, A. Gazivoda, M. Madzarac, *Electrochim. Acta*, 47 (2002)4189.
24. M. Sahin, S. Bilgic, H. Yilmaz*, Appl. Surf. Sci.*, 195 (2002) 1.
25. S. M. Abd El Haleem, S. Abd El Wanees, E.E.Abd ElAal, A, Farouk, *Corros. Sci.*, 68(2013)1.
26. E. E. Abd El Aal, S. Abd El Wanees, S. M. Abd El Haleem, A., Farouk, *Corros. Sci.*, 68(2013)14.
27. M. Abdallah, H. M. Al-Tass, B.A. Al Jahdaly, A.S. Fouda, *J. Mol. Liq.*, 216 (2016)590.
28. A. M. Fekry, M. A. Ameer, *Int. J. Hydrogen Energy*, 36 (2011) 11207.
29. A.S. Fouda, S. El-Din H. Etaiw, M. M. El-bendary, M,M. Maher, *J. Mol. Liq.*, 213 (2016) 228.
30. S. Kerte, B. Hammouti, *Appl. Surf. Sci.*, 93 (1996) 59.
31. X. Li, S. Deng, H. Fu, T. Li, Electrochim. Acta, 54 (2009)89.
32. K. Shalabi, Y. A. Abdallah, Hala M. Hassan, A.S. Fouda, *Int. J. Electrochem. Sci.*, 9 (2014) 1468.
33. M. Lebrini, M. Lagrenee, H. Vezin, M. Traisnel, F. Bentiss, *Corros. Sci.*, 49(2007)2254.
34. . I.B. Obot, N.O Obi-Egbedi, S. A. Umoren, Corros. Sci., 51 (2009)276.
35. P. X. Hui, G. Min, Z. Yu Xuan, W.Qin, H. B. Rong, Sci. China, Ser. B:Chem. (2011)4332.
36. T. Hong, W. P. Jepson, *Corros. Sci.*, 43 (2001) 1839.
37. A. P. Yadav, A. Nishikata, T. Tsuru, *Corros. Sci.*, 46 (2004) 169.
38. K. F. Khaled, *Appl. Surf. Sci.*, 252 (2006) 4120.
39. S. M. Abd El Haleem, S. Abd El Wanees, A, Baghat, *Corros. Sci.*, 87(2014)321.
40. M.M. Solomon, S.A. Umoren, I.I. Udosoro, A.P. Udoh, *Corros. Sci.*, 52 (2010) 1317.
41. A.A. Gürten, K. Kayakırılmaz, M. Erbil, *Constr. Build. Mater*, 21 (2007) 669.
42. A. Khamis, M. M. Saleh, M. I. Awad and B.E. El-Anadouli, *Corros. Sci.*, 74(2013)83.
43. H. B. Rudresh and S. M. Mayanna, *J. Environ. Sci. Technol.*, 122 (1977) 25.
44. N. Guan, M. L. Xueming, L. Fei, *Mater. Chem. Phys.*, 86 (2004)59.
45. A. K. Singh, E. E. Ebenso, *Int. J. Electrochem. Sci.*, 7(2012) 2349.
46. H. Luo, Y.C. Guan, K.N. Han, *Corrosion NACE*, 54 (1998) 619.
47. C.A. Miller, S. Qutubuddin, in: H.F. Eick, C.D. Parfitt (Eds.), Interfacial Phenomena in Apolar Media, Surfactant Science Series, vol. 21, Markel Dekker Inc., New York, Basel, 1987, p. 166.
48. O. Olivares, N.V. Likhanova, B. Gomez, J. Navarrete, M.E. Llanos-Serrano, E. Arce, J.M. Hallen, *Appl. Surf. Sci.*, 252 (2006) 2894.
49. S. Trasatti, *Electrochim. Acta*, 37 (1992) 2137.
50. A.Popova, E. Sokolova, S. Raicheva, M. Christov, *Corros. Sci.*, 45 (2003) 33.
51. A.S. Fouda, Y.A. Elewady, H.K. Abd El-Aziz and A.M.Ahmed, *Int. J. Electrochem. Sci.*, 7 (2012) 10456.
52. X. Li, S. Deng, G. Mu, H. Fu and F. Yang, *Corros. Sci.*, 50(2008)420.